Coordination Chemistry of SCS Pd^{II} Pincer Systems

Henk-Jan van Manen,[a] Kazuaki Nakashima,[a,b] Seiji Shinkai,[b] Huub Kooijman,[c] Anthony L. Spek,[c][‡] Frank C. J. M. van Veggel,*[a] and David N. Reinhoudt*[a]

Keywords: Coordination chemistry / N ligands / P ligands / Palladium / Tridentate ligands

We have studied the coordination of substituted pyridines, and phosphorus- and sulfur-containing ligands to an SCS Pd^{II} pincer system. These ligands coordinate to Pd^{II} (*trans* to the cyclopalladated aryl group) by quantitative substitution of the labile acetonitrile ligand in complex **1**. Competition experiments showed that both electronic and steric effects influence the strength of coordination to the Pd^{II} pincer of the substituted pyridines. A quantitative analysis of the substituent effect was achieved by a Hammett correlation. Phosphorus-containing ligands also coordinate to this SCS Pd^{II} motif, as evidenced by NMR spectroscopy and single-crystal X-ray diffraction studies. They are much stronger ligands than the pyridines. The coordination strength of the thioureas falls in between those of the pyridines and phosphanes/phosphites. Our results lead therefore to the following order of ligand strength towards Pd^{II} in SCS Pd^{II} pincers: $PR_3 > P(OR)_3 > N,N'$-disubstituted thiourea > (substituted) pyridines > MeCN.

Introduction

meta-Xylene derivatives in which the two methylene groups carry suitable donor atoms (e.g. N, P, or S), so-called pincer ligands,[1] are used for the complexation of a wide range of transition metals.[2] Cyclometallation gives rise to a variety of systems displaying rich coordination chemistry.

A number of stable Pd^{II} complexes containing SCS pincer systems have been reported to date,[3] with recent examples mainly related to supramolecular chemistry.[4] We have been exploiting the SCS Pd^{II} pincer motif in the noncovalent synthesis of nanosize metallodendrimers.[5] Representative dendritic building blocks used in our investigations are depicted in Scheme 1.

Controlled metallodendrimer assembly up to generation 5 has been achieved by *divergently* growing from the core $\mathbf{G_0}$.[6] In these metallodendritic structures, the coordination of nitrile ligands is used as the assembling principle. Large self-assembled hyperbranched organopalladium spheres (100−400 nm) have also been synthesized divergently by an uncontrolled one-pot strategy.[7]

By employing ligands of different coordination strengths, it is also possible to synthesize metallodendrimers in a *convergent* manner.[8] This growth strategy commences by coordinating the strongest ligands first (at the periphery). Subsequent growth proceeds inwards using building blocks of decreasing coordination strength. This order is imperative in preventing ligand scrambling. We have demonstrated this type of growth in the synthesis of a third generation metallodendrimer containing cyano- and pyridine-based building blocks. In order to broaden the scope of this metallodendrimer synthetic method, other ligands with different binding strengths are needed. Therefore, we have studied the relative coordination strengths of a series of ligands towards

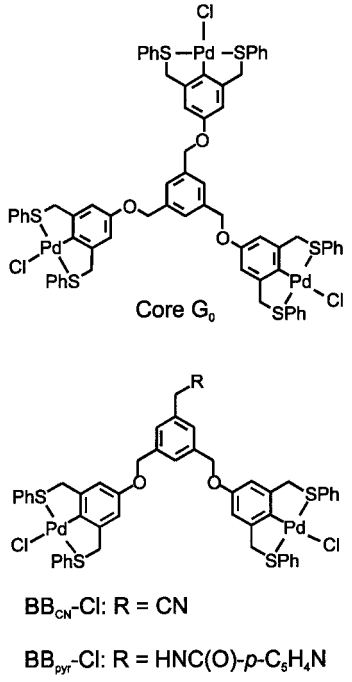

Scheme 1. Representative building blocks that have been employed to assemble metallodendrimers, see refs.[6−8]

[a] Laboratory of Supramolecular Chemistry and Technology, MESA+Research Institute, University of Twente,
P. O. Box 217, 7500 AE, Enschede, The Netherlands
Fax: (internat.) + 31-53/4894645
E-mail: smct@ct.utwente.nl
[b] Chemotransfiguration Project, Japan Science and Technology Corporation,
2432 Aikawa, Kurume, Fukuoka 839-0861, Japan
[c] Bijvoet Center for Biomolecular Research, Department of Crystal and Structural Chemistry, Utrecht University,
Padualaan 8, 3584 CH Utrecht, The Netherlands
[‡] To whom correspondence pertaining to crystallographic studies should be addressed (E-mail: a.l.spek@chem.uu.nl)

  1434−1948/00/1212−2533 $ 17.50+.50/0

the SCS Pd^{II} pincer system. We report here our results for the parent Pd^{II} pincer. Moreover, a dipincer has been synthesized which could be used as a new rigid core for metallodendrimer synthesis.

Results and Discussion

Synthesis and Characterization of Model SCS Pd^{II} Pincer Complexes

The SCS Pd^{II} complexes **1** and **2** were prepared in two and three steps, respectively (Scheme 2). After alkylation of the previously reported[7b] SCS pincer ligand **4** with *n*-butyl bromide (77% yield), cyclopalladation of the resulting ligand **5** was achieved by reaction with $[Pd(CH_3CN)_4][BF_4]_2$.

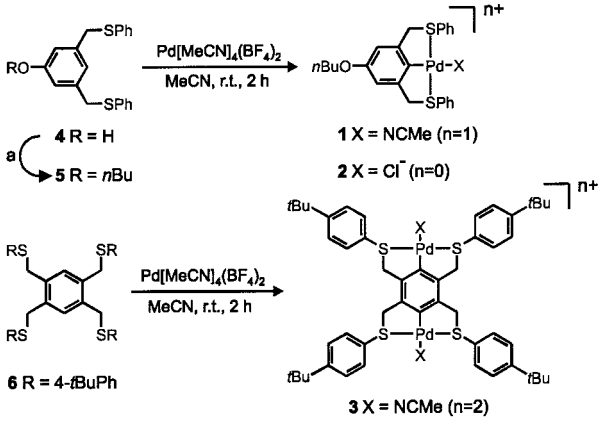

Scheme 2. Synthesis of SCS Pd^{II} pincer complexes; a) *n*BuBr, *t*BuOK, CH_3CN

The cationic acetonitrile complex **1** (containing the noncoordinating BF_4^- counter anion) was obtained in 90% yield by precipitation with Et_2O from CH_3CN solution after completion of the cyclopalladation. The neutral chloro complex **2** was isolated (in 94% yield) by stirring a solution of **1** in CH_2Cl_2/CH_3CN with saturated NaCl, followed by column chromatography.

Similarly, dipincer **3** was prepared in two steps from 1,2,4,5-tetrakis(bromomethyl)benzene by first allowing the benzyl bromides to react with *tert*-butylthiophenol using K_2CO_3 as base and 18-crown-6 as catalyst (81% yield), followed by cyclopalladation of the resulting dipincer ligand **6** using $[Pd(CH_3CN)_4][BF_4]_2$ in CH_3CN. The bis(acetonitrile) complex was purified by precipitation from CH_3CN solution with Et_2O (60% yield). Complexes **1**, **2** and **3** were isolated as air- and moisture-stable yellow solids. All spectroscopic and analytical data are consistent with cyclopalladation. Compared to the free ligands **5** and **6**, the ^1H NMR resonances for the diastereotopic CH_2S protons in the palladium complexes are shifted downfield by ca. 0.5 ppm and are broadened due to slow conformational interconversion of the Pd^{II}-containing five-membered rings. At lower temperatures the coupling of the two diastereotopic CH_2S protons results in the broad signal splitting into a pair of doublets (vide infra). Further, the signals for the *ortho*-protons at $\delta = 6.80$ (in **5**) or $\delta = 6.92$ (in **6**) are absent from the ^1H NMR spectra, indicating complete cyclopalladation. In the ^{13}C NMR spectra of the acetonitrile complexes **1** and **3**, the signal of the carbon atom directly linked to Pd^{II} is too weak to be observed (probably due to long relaxation times), whereas in the chloro complex **2** it is present at $\delta = 150.9$ (30 ppm downfield compared to ligand **5**). In the positive FAB-MS spectrum of **2**, a signal corresponding to $[M - Cl + H]^+$ ($m/z = 499.6$) is present, whereas in the negative FAB-MS spectrum the chloride ion remains coordinated to Pd^{II}, resulting in a signal at $m/z = 533.7$ ($[M]^+$). Loss of the acetonitrile ligand is observed in both the positive and negative FAB-MS spectra of **1**, resulting in signals corresponding to $[M - MeCN - BF_4]^+$ ($m/z = 499.0$) and $[M - MeCN + BF_4]^-$ ($m/z = 671.6$) respectively, while both acetonitriles are lost in the positive FAB-MS spectrum of **3** ($m/z = 1001.1$ for $[M - 2MeCN - 2BF_4 + H]^+$).

X-ray Structure of 1

Besides the analytical evidence discussed above, structural proof of the acetonitrile complex **1** is provided by an X-ray analysis. A drawing of the acetonitrile complex **1** is shown in Figure 1. The following bond lengths for the atoms bonded to Pd^{II} have been obtained: Pd−S(1) 2.2992(8) Å, Pd−S(2) 2.2961(9) Å, Pd−N 2.110(2) Å, Pd−C(1) 1.975(2) Å.

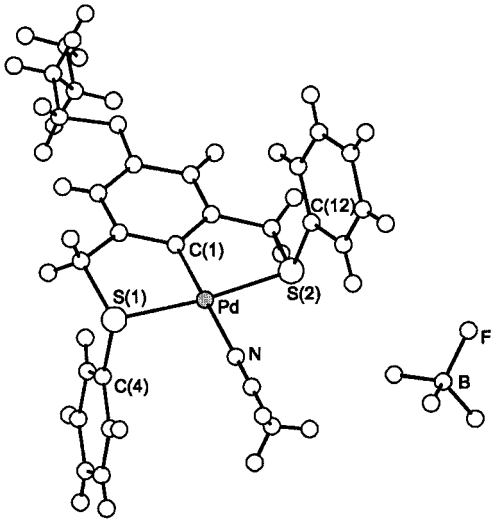

Figure 1. Structure of the acetonitrile complex **1**

The Pd atom adopts a slightly distorted square-planar geometry [S(1)−Pd−S(2) 171.11(2)° and N−Pd−C(1) 178.26(11)°] and the two five-membered chelate rings possess somewhat distorted envelope conformations in which the two phenyl rings (oriented *anti* with respect to the square plane) are in axial positions [Pd−S(1)−C(4) 100.51(9)° and Pd−S(2)−C(12) 103.17(9)°]. It should be noted that complex **1** is chiral in the solid state (prepared as a racemate) due to the lack of symmetry elements.

Substitution of the Labile MeCN Ligand by Pyridine

Substitution of the labile acetonitrile ligand of complex **1** by stronger ligands such as pyridine is facile. Upon treat-

ment of **1** with 1 equiv. of pyridine (in $CDCl_3$), fast and quantitative substitution was observed. In the ^1H NMR spectrum of the pyridine adduct, the resonance of the pyridine α-protons is shifted *upfield* from δ = 8.60 (free pyridine) to δ = 8.15 (coordinated pyridine). This is different from the pyridine complexes of SCS Pd^{II} pincers reported by Loeb and co-workers[9] for which a *downfield* shift of the pyridine α-protons was observed upon coordination. This difference must be due to the presence of the phenyl rings attached to the sulfur atoms in our system. The ring current of these aromatic rings will have a shielding effect on the pyridine protons (mostly the α-protons). The α-proton signal is also considerably broadened, indicating hindered rotation of the pyridine ligands with respect to the plane of coordination. The CH_2S proton signal shifts downfield by 0.15 ppm, and the aromatic proton signal by 0.05 ppm, upon substitution of MeCN by pyridine. The greater coordination strength of the pyridine ligand as compared to acetonitrile is also evident from the positive FAB-MS spectrum, in which a small, but significant peak corresponding to the molecular ion $[M - BF_4]^+$ is observed at *m*/*z* = 578.4, in addition to a large signal at *m*/*z* = 499.2 from $[M - pyr - BF_4]^+$.

Upon adding excess pyridine, two separate NMR signals for free and bound pyridine are observed. This observation can be explained by either slow exchange of pyridine on the NMR timescale or a kinetically stable pyridine complex. Exchange of pyridine was indeed evidenced by treatment of the pyridine complex with an excess (5 equiv.) of $[D_5]$pyridine. The signal at δ = 8.15 disappeared and a new peak appeared at δ = 8.6, indicating free pyridine. This kinetic lability is consistent with other pyridine−Pd^{II} complexes.[10]

The pyridine exchange rate is dependent on the solvent. In $CDCl_3$ two separate signals for bound and free pyridine were observed up to 50 °C. However, when acetonitrile complex **1** was treated with 2 equiv. of pyridine in $[D_6]$DMSO, a coordinating solvent, only one broad signal for the pyridine α-protons was observed in the ^1H NMR spectrum, indicating fast exchange on the NMR timescale. When $[D_6]$DMSO was titrated into a $CDCl_3$ solution of the pyridine complex containing 1 equiv. of excess pyridine (Figure 2), the rate of pyridine exchange varied with the concentration of $[D_6]$DMSO.

It is known that the kinetics of substitution in d^8 square-planar complexes depends on two factors, one related to direct ligand attack (associative-dissociative mechanism) and the other to an associative solvolysis pathway, in which the leaving group is first displaced by a solvent molecule and which is subsequently substituted by the incoming ligand (dissociative-associative mechanism).[11] The observed pyridine exchange rate can be rationalized in this way. With increasing $[D_6]$DMSO concentration, the pyridine exchange increasingly follows the solvolysis pathway. In $CDCl_3$ this pathway is not possible and only slow direct pyridine attack occurs.

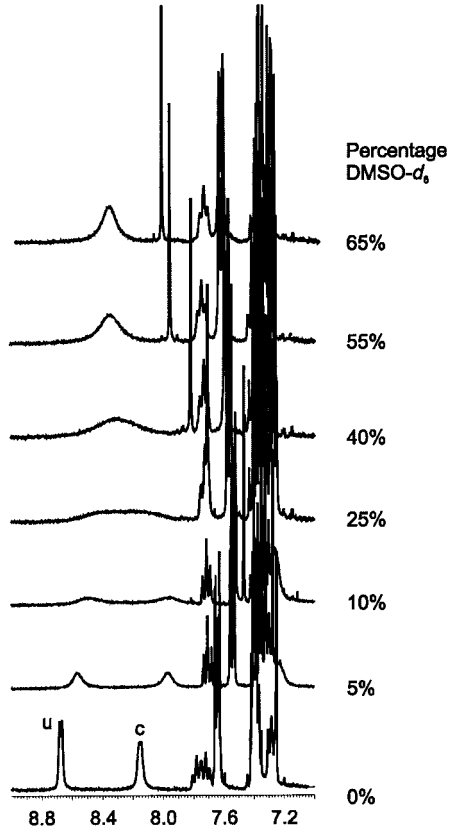

Figure 2. ^1H NMR spectra (298 K) of the titration of $[D_6]$DMSO to a $CDCl_3$ solution of the pyridine complex of the SCS Pd^{II} pincer system containing an excess of 1 equiv. pyridine; the designations u and c correspond to the pyridine α-proton signals of uncoordinated and coordinated pyridine, respectively

Substituent Effects on Pyridine Complex Stability

Within a series of substituted pyridines, we anticipated that subtle differences in nitrogen electron density would control the coordination strength towards Pd^{II}. When two different pyridines (each 1 equiv.) were mixed with 1 equiv. of the acetonitrile complex **1** in $CDCl_3$ (Scheme 3), the α-proton signals of the two pyridines in the ^1H NMR spectra were used as a probe to determine the extent of coordination of each pyridine (e.g. see Figure 3).

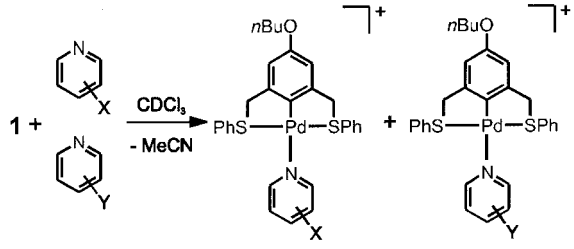

Scheme 3. Competition experiments between substituted pyridines

Table 1 shows that electron-donating pyridines bind more strongly than pyridine, whereas electron-withdrawing pyridines are weaker ligands than pyridine. The stability of these pyridine complexes follows the Hammett equation using the σ^+ constant of Brown and Okamoto.[13] This modified substituent constant applies to reactions in which strong ac-

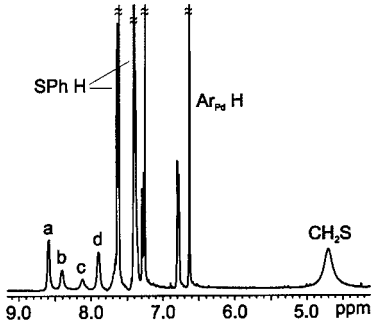

Figure 3. Part of the ^{1}H NMR spectrum ($CDCl_3$, 298 K) for a competition experiment between pyridine and 4-methoxypyridine. The designated signals correspond to the pyridine α-proton signals of: a) free pyridine, b) free 4-methoxypyridine, c) bound pyridine, d) bound 4-methoxypyridine

ceptor character develops at the aromatic ring, e.g. solvolysis of tertiary halides in which ionization is rate-determining. Using the selectivities reported in Table 1 (only the data of the 4-substituted pyridines are analyzed), a Hammett plot as shown in Figure 4 is obtained with a ρ^+ value of -1.0.

Table 1. Results of coordination competition experiments between substituted pyridines

X	Y	% bound pyr−X/pyr−Y	Selectivity[a]
4-H	4-NH_2	17:83	4.88
4-H	4-MeO	32:68	2.13
4-H	4-*t*Bu	40:60	1.50
4-H	4-Me	45:55	1.22
4-H	4-Ph	44:56	1.27
4-H	4-Ac	62:38	0.61
4-H	4-CO_2Me	64:36	0.56
2-Me	4-Me	43:57	1.33
2-Me	3-Me	57:43	0.75

[a] Ratio of bound pyridine−Y over bound pyridine−X.

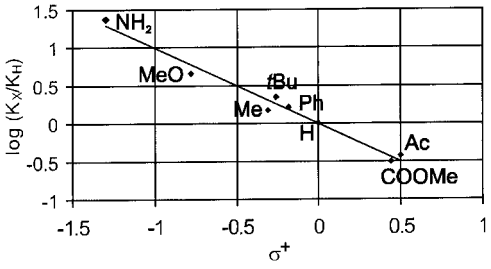

Figure 4. Hammett plot of the stability of 4-substituted pyridine complexes with the SCS Pd^{II} pincer system against the Brown−Okamoto σ^+ substituent constant

Usually in systems obeying the Brown−Okamoto equation, the values of ρ^+ are much more negative. However, in those cases a full positive charge develops in the rate-determining step instead of the partial positive charge developing on nitrogen in pyridine−Pd^{II} coordination.

The effect of steric hindrance was investigated in the picoline series. On the basis of electronic effects alone, it would be expected that 2-picoline would bind stronger than 3-picoline. However, as the reverse is found experimentally, it must be concluded that steric hindrance between the 2-methyl group and the aryl groups of the Pd^{II} pincer system overrules electronic effects in this case.

Coordination of Triphenylphosphane to Pd^{II}

The coordination of phosphorus-containing ligands to SCS Pd^{II} pincers has, to the best of our knowledge, not been investigated. Only phosphanes coordinated to transition metal pincer systems of the PCP[14] and NCN[15] type, and a phosphane coordinated to an SCS Pt^{II} pincer[3] have been reported. Upon addition of 1 equiv. of PPh_3 to **1**, several distinct spectroscopic features evidenced phosphane coordination to Pd^{II}. Firstly, in the ^{1}H NMR spectrum a broad peak corresponding to the CH_2S protons is present. The signal is sharper and is shifted downfield (± 0.25 ppm) when compared to the MeCN complex. Furthermore, the signal from the aromatic protons is a doublet (J = 2.9 Hz) due to proton-phosphorus coupling. In the ^{31}P NMR spectrum, the phosphorus signal shifts from δ = −5.6 (free PPh_3) to δ = 13.6 upon coordination. These combined results prove the coordination of PPh_3 *trans* to the cyclometallated aryl group. Opening of the S−Pd chelate ring, as suggested by Shaw et al.,[16] does not occur.

X-ray Structure of 3·$(PPh_3)_2$

The *dipincer* complex **3**, which is more soluble in organic solvents than reported dipincers[17] due to its *tert*-butyl groups, was mixed with 2 equiv. of PPh_3. Crystals were grown by vapor diffusion of diethyl ether into a $CHCl_3$ solution of the bis(PPh_3) complex (Figure 5).

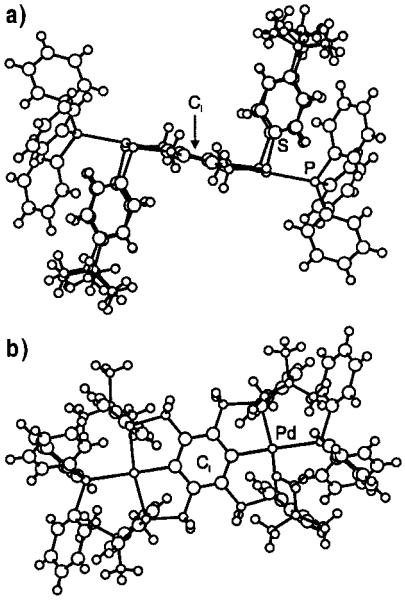

Figure 5. Structure of 3·$(PPh_3)_2$; a) side view, b) top view

In the bis(triphenylphosphane) complex, the Pd atoms are in a distorted square-planar environment: S(1)−Pd(1)−S(2) 167.15(3)° and P(1)−Pd(1)−C(1) 178.53(9)°. The following bond lengths for the atoms bon-

ded to Pd^{II} were obtained: Pd−S(1) 2.3075(10) Å, Pd−S(2) 2.3057(9) Å, Pd−P 2.3785(9) Å, Pd−C(1) 2.032(3) Å. The Pd^{II}−C bond is substantially longer than in complex **1** (2.03 vs. 1.98 Å). The complex has C_i symmetry (inversion point at the center of the bispalladated ring) in which the two *tert*-butyl phenyl groups attached to the metal-bound sulfur atoms of the same SCS Pd^{II} pincer moiety are oriented towards the same side of the square plane.

Stability of Coordinated PPh_3 Complexes

In transition metal inorganic complexes, PPh_3 is in general a stronger ligand than pyridine. This is expressed in their respective nucleophilicity parameters, for example, which differ substantially (n^0_{Pt} = 3.19 for pyridine and 8.93 for PPh_3, respectively).[11] In the ^1H NMR spectrum of a mixture of 1 equiv. of PPh_3 and the pyridine complex of compound **1** (Scheme 2: X = pyridine), quantitative substitution of pyridine by PPh_3 is shown. The spectrum is a superposition of the spectra of free pyridine and the PPh_3 complex. Heating the PPh_3 complex in refluxing $CHCl_3$ with a 10-fold excess of pyridine did not result in any detectable exchange.

As mentioned before, ring opening of the S−Pd chelate by PPh_3 has been suggested. Upon adding 5 equiv. of PPh_3 to *acetonitrile* complex **1**, no changes were observed in either the ^1H or ^{31}P NMR spectra. The situation was different when PPh_3 was added to the *chloro* complex **2**. Increasing amounts (0.25, 0.5, 1.0, 1.5, 2.5 and 5.0 equiv.) of PPh_3 were added to **2**. The ^1H and ^{31}P NMR spectra show that an equilibrium is established after each addition because in every case two signals are observed in the ^{31}P NMR spectrum, one corresponding to free PPh_3 ($\delta = -5.6$), and the other indicating coordination of PPh_3 *different from that described for the substitution of acetonitrile above* because the signal of coordinated PPh_3 now appears at $\delta = 21.9$ instead of $\delta = 13.6$. In the ^1H NMR spectrum a signal appears that corresponds to "free" CH_2S protons. This means that *the S−Pd chelate ring opens upon PPh_3 addition*. It also seems that both chelate rings open together, as the opening of only one would destroy the symmetry of the system. Substitution of the chloro ligand by PPh_3 is also unlikely, as can be inferred from the ^{31}P NMR spectra (i.e. no signal observed at $\delta = 13.6$). Therefore it is concluded that 2 molecules of PPh_3 displace the sulfur atoms as ligands. This only occurs quantitatively with a large excess (> 4−5 equiv.) of PPh_3.

Coalescence Temperatures of Different SCS Pd^{II} Pincer Complexes

The two five-membered chelate rings of the cyclopalladated pincer system display slow conformational interconversion, which is reflected in the ^1H NMR spectrum by the broadening of the CH_2S proton signal of the pincer complexes. Different ligands have a different influence on the conformational interconversion of the chelate rings. This phenomenon is reflected in the coalescence temperature T_c where the two *separate* signals of the CH_2S protons coalesce into a broad singlet.

As can be seen from Table 2, the coalescence temperature decreases in the order acetonitrile > pyridine > chloride > triphenylphosphane. For the neutral ligands this order corresponds to the lone pair electron donation (the nucleophilicity) towards Pd^{II}. In the case of PPh_3, no unambiguous coalescence temperature could be observed. NMR experiments at low temperatures reveal multiple signals for the CH_2S protons for all the complexes mentioned above. On one hand, freezing out the ring puckering results in loss of the apparent C_{2v} symmetry of the complex that exists at higher temperatures in solution. On the other hand, in the PPh_3 complex one very broad signal is observed, ranging from $\delta = 4.3$ to $\delta = 5.2$ at −10 °C. Splitting of the signal into two doublets is not observed, suggesting that besides lowering the rate of ring interconversion, rotation of the bulky PPh_3 ligand around the Pd^{II}−P bond is also restricted, leading to different conformational isomers. Moreover a long range coupling to ^{31}P cannot be excluded a priori.

Table 2. Coalescence temperatures and free energies of activation for ring interconversion of SCS Pd^{II} pincer complexes

Ligand X	Coalescence temperature T_c [K]	Free energy of activation $\Delta G^{\ddagger}_c$ [kJ/mol] at T_c
MeCN	289 ± 2	57.5 ± 0.3
Pyridine	286 ± 2	56.5 ± 0.3
Cl^-	271 ± 2	54.8 ± 0.5
PPh_3	< 268[a]	−

[a] No unambiguous coalescence temperature was observed, see also text.

From the coalescence temperature the free energy of activation for ring puckering can be estimated.[12] The free energies of activation for ring puckering vary between 55 and 58 kJ/mol in the ligand order chloride < pyridine < acetonitrile. From Table 2 it is evident that higher coalescence temperatures correspond to higher free energies of activation at T_c for ring puckering in this system.

Coordination of Other Phosphorus-Containing Ligands

Besides triphenylphosphane other phosphorus-containing ligands were investigated as ligands for the SCS Pd^{II} pincer system. Coordination of these ligands to Pd^{II} was shown by ^1H and ^{31}P NMR spectroscopy and by FAB mass spectrometry (Table 3).

As with the substituted pyridines competition experiments were employed, establishing that the relative coordination strengths of these ligands increase in the order $PCy_3 > PPh_3 > P(OMe_3) > P(OPh)_3$. The relative differences in coordination strengths are quite high, as in all cases [PCy_3 vs. PPh_3, PPh_3 vs. $P(OMe)_3$ and $P(OMe)_3$ vs. $P(OPh)_3$] the selectivity exceeds a 4:1 ratio. Further competition experiments revealed that all the phosphorus containing ligands coordinate much more strongly than pyrid-

Table 3. Complexes of phosphorus-containing ligands with the SCS Pd^{II} pincer system

Complex **1** with X =	^{1}H NMR Ar H[a] (ppm)/*J* (Hz)	^{31}P NMR coord/free ligand (ppm)	FAB-MS $[M]^+$ found/calcd
$P(OMe)_3$	6.72/4.8	122.7/141.0	623.2/623.1
$P(OPh)_3$	6.64/5.1	114.7/127.9	809.1/809.1
PCy_3	6.66/2.9	24.0/11.5	779.5/779.3

[a] Aromatic protons of cyclopalladated ring.

ine. Only a minor amount of pyridine complex was found in competition experiments with the weakest phosphite ligand [$P(OPh_3)$].

In the case of PCy_3 and $P(OPh)_3$, addition of excess ligand to their respective phosphane or phosphite complexes had no effect on the complex stability, as was the case for PPh_3 (vide supra). However, upon addition of excess $P(OMe)_3$ to complex **1** [X = $P(OMe)_3$], the SPh ligands were substituted by $P(OMe)_3$ to form a complex containing three phosphite ligands. This was evidenced by ^{1}H (the CH_2S protons give a sharp signal at $\delta = 4.2$) and ^{31}P NMR spectroscopy (the two *trans* phosphite ligands couple to the *cis* phosphite ligand and vice versa to give one triplet and one doublet, $J = 73$ Hz). In the other cases the presence of one bulky ligand apparently prevents the coordination of additional ligands.

The observed order of phosphorus ligand strengths matches the order of χ_i values [$\chi_i = 0.1$ (Cy), 4.3 (Ph), 7.7 (OMe) and 9.7 (OPh)], which is regarded as a parameter measuring substituent contribution to the σ donor and π acceptor abilities of phosphorus-containing ligands.[18] On the other hand, the cone angle θ (the ligand bulkiness) increases in the order $P(OMe)_3$ (107°) < $P(OPh)_3$ (128°) < PPh_3 (145°) < PCy_3 (170°).[18] Obviously in our case steric effects can be ignored, as the ligand strength order is the same as the electronic parameter χ_i and not the steric parameter θ.

Coordination of Sulfur-Containing Ligands

Finally, we have investigated the coordination of sulfur-containing ligands to the SCS Pd^{II} pincer. Thioureas have high nucleophilicity values ($n^0_{Pt} = 7.17$ for unsubstituted thiourea),[11] so they are possible ligands.[19] *N*-Benzyl-*N*′-butylthiourea was prepared from butyl isothiocyanate and benzylamine. Upon addition of this thiourea to the acetonitrile complex **1**, the ^{1}H NMR spectrum indicated thiourea coordination. Firstly, the acetonitrile signal was present at $\delta = 1.99$, indicating the release of acetonitrile (coordinated MeCN gives rise to a signal at $\delta = 2.08$). Secondly, significant changes in the chemical shifts of the thiourea NH protons and the adjacent CH_2 protons were observed. Finally, the broad signals of the SPh protons of the pincer and essentially all protons of the thiourea indicated restricted thiourea rotation. Moreover, the FAB-MS spectrum displayed an intense signal at $m/z = 721.2$ corresponding to the thiourea complex.

From their n^0_{Pt} values we can expect that thioureas are stronger ligands than pyridine but weaker ligands than phosphanes. This was confirmed experimentally by competition experiments. The ^{1}H NMR spectra show that the ratio of coordinated thiourea to coordinated pyridine is higher than 95:5. In the presence of PPh_3 the thiourea did not coordinate significantly, as was inferred from ^{1}H and ^{31}P NMR spectroscopy. FAB mass spectrometry only showed the PPh_3 complex of the SCS Pd^{II} pincer system in such mixtures. This means that the order of ligand strength is PPh_3 > thiourea > pyridine.

Conclusions

In this paper, a study of the coordination strengths of various ligands towards a SCS Pd^{II} pincer system has been reported. Several *para*-substituted pyridines have been coordinated to this pincer system, and the differences in coordination strengths found to arise from electronic and steric effects. The effect of *para* substituents was quantitatively analyzed by correlation with the Brown−Okamoto σ^+ substituent constants. Moreover, it was demonstrated that phosphorus- and sulfur-containing ligands are stronger ligands than pyridines. These results allow for the *convergent* metallodendrimer assembly methodology to be extended. Investigations concerning these topics are currently underway and the results will be described elsewhere.

Experimental Section

General: Melting points were determined with a Reichert melting point apparatus and are uncorrected. CH_2Cl_2 and hexane were freshly distilled from $CaCl_2$. CH_3CN (p.a. from Merck) was stored over molecular sieves (4 Å). Other solvents (EtOH, $CHCl_3$, acetone) were used as received (p.a. from Merck). All reagents were purchased from Aldrich and used without further purification. Solutions containing phosphanes or phosphites were degassed prior to use. − NMR spectra were recorded in $CDCl_3$ (unless stated otherwise) at 298 K with a Varian Unity 300 locked to the deuterated solvent. Chemical shifts are given relative to tetramethylsilane (TMS). − FAB-MS spectra were recorded with a Finnigan MAT 90 spectrometer with *m*-nitrobenzyl alcohol (NBA) as the matrix. − Elemental analyses were performed using a Carlo Erba EA1106. − Column chromatography was performed using silica gel (SiO_2, E. Merck, 0.040−0.063 mm, 230−240 mesh).

1-(*n*-Butoxy)-3,5-bis(phenylthiomethyl)benzene (5): To a solution of 3,5-bis(phenylthiomethyl)phenol (**4**) (1.40 g, 4.1 mmol) in CH_3CN (200 mL) was added *t*BuOK (0.93 g, 8.3 mmol) and the resulting mixture was stirred at room temperature for 1 h. A solution of *n*-butyl bromide (0.44 mL, 4.1 mmol) in CH_3CN (20 mL) was added

dropwise, and the mixture was stirred overnight at 40 °C. After evaporation of the solvent in vacuo, the residue was taken up in CH_2Cl_2 (100 mL), washed with 1 M HCl (100 mL), saturated $NaHCO_3$ (100 mL) and brine (100 mL). The dried ($MgSO_4$) organic layer was concentrated to dryness and the crude product was purified by column chromatography (SiO_2; eluent: CH_2Cl_2/hexane, 1:1, v/v) to afford a colorless oil. Yield: 1.26 g (77%). − ^{1}H NMR: δ = 0.94 (t, J = 7.3 Hz, 3 H, CH_3), 1.36−1.51 (m, 2 H, CH_2CH_3), 1.63−1.74 (m, 2 H, OCH_2CH_2), 3.83 (t, J = 6.6 Hz, 2 H, OCH_2), 4.01 (s, 4 H, CH_2S), 6.68 (s, 2 H, Ar H), 6.80 (s, 1 H, Ar H), 7.12−7.29 (m, 10 H, SPh). − ^{13}C NMR: δ = 13.3, 18.7, 30.7, 38.5, 67.1, 113.4, 121.1, 125.8, 128.3, 129.4, 135.8, 138.5, 158.8. − FAB-MS; *m/z*: 395.1 $[M + H]^+$, calcd. for $C_{24}H_{26}OS_2$: 395.1.

Acetonitrile Complex of Pd Pincer 1: Ligand **5** (233 mg, 0.6 mmol) was dissolved in CH_3CN (50 mL) and the solution was placed under argon. $Pd[MeCN]_4(BF_4)_2$ (262 mg, 0.6 mmol) was added in one portion, and the mixture was stirred at room temperature for 2 h. After evaporation of the solvent in vacuo, the yellow paste was taken up in CH_3CN (3 mL) and the product was precipitated by dropwise addition of diethyl ether. Yield: 334 mg (90%). − M.p. 68−70 °C. − ^{1}H NMR: δ = 0.95 (t, J = 7.3 Hz, 3 H, CH_3), 1.37−1.52 (m, 2 H, CH_2CH_3), 1.67−1.76 (m, 2 H, OCH_2CH_2), 2.08 (s, 3 H, CH_3CN), 3.88 (t, J = 6.4 Hz, 2 H, OCH_2), 4.57 (br s, 4 H, CH_2S), 6.59 (s, 2 H, Ar H), 7.48−7.50 (m, 6 H, SPh), 7.77−7.81 (m, 4 H, SPh). − ^{13}C NMR (CD_3CN): δ = 13.6, 19.4, 31.4, 50.3, 68.2, 110.2, 130.6, 131.3, 131.5, 132.1, 151.8, 158.2. − FAB-MS; *m/z*: 499.0 $[M - BF_4 - CH_3CN]^+$, calcd. 499.0. − $C_{26}H_{28}BF_4NOPdS_2 \cdot H_2O$: calcd. C 48.35, H 4.68, N 2.17, S 9.93; found C 48.18, H 4.50, N 2.25, S 9.92.

Chloro Complex of Pd Pincer 2: Acetonitrile complex **1** (0.75 g, 1.2 mmol) was dissolved in a mixture of CH_2Cl_2 (75 mL) and CH_3CN (25 mL). After the addition of brine (100 mL), the mixture was stirred vigorously overnight. After separation of the layers, the organic phase was concentrated in vacuo and the residue was purified by column chromatography (SiO_2; eluent: CH_2Cl_2/Et_2O, 95:5, v/v) to afford a yellow solid. Yield: 0.60 g (94%). − M.p. 63−64 °C. − ^{1}H NMR: δ = 0.94 (t, J = 7.3 Hz, 3 H, CH_3), 1.40−1.48 (m, 2 H, CH_2CH_3), 1.66−1.75 (m, 2 H, OCH_2CH_2), 3.85 (t, J = 6.4 Hz, 2 H, OCH_2), 4.53 (br s, 4 H, CH_2S), 6.56 (s, 2 H, Ar H), 7.32−7.37 (m, 6 H, SPh), 7.78−7.83 (m, 4 H, SPh). − ^{13}C NMR: δ = 13.3, 18.7, 30.8, 51.2, 67.3, 108.3, 129.1, 129.2, 130.9, 131.9, 149.6, 150.9, 156.5. − FAB-MS; *m/z*: 499.6 $[M - Cl + H]^+$, calcd. 500.0. − $C_{24}H_{25}ClOPdS_2$: calcd. C 53.83, H 4.71, S 11.98; found C 53.90, H 4.70, S 11.88.

Dipincer Ligand 6: A mixture of 1,2,4,5-tetrakis(bromomethyl)benzene (3.00 g, 6.7 mmol), 4-*tert*-butylthiophenol (5.00 g, 30.1 mmol), K_2CO_3 (9.20 g, 66.6 mmol) and 18-crown-6 (1.80 g, 6.8 mmol) in acetone (150 mL) was heated at reflux overnight under argon. After evaporation of the solvent, the residue was taken up in CH_2Cl_2 (250 mL) and washed with brine (250 mL). After drying the organic layer with $MgSO_4$ and evaporation of the solvent in vacuo, the crude product was recrystallized from $EtOH/CHCl_3$ to afford a white solid. Yield: 4.30 g (81%). − M.p. 185−186 °C. − ^{1}H NMR:

Table 4. Crystallographic data for **1** and **3**·$(PPh_3)_2$

	1	**3**·$(PPh_3)_2$
Empirical formula	$C_{26}H_{28}NOPdS_2 \cdot BF_4$	$C_{86}H_{90}P_2Pd_2S_4 \cdot 2BF_4 \cdot 2CHCl_3$
Molecular mass	627.86	1939.07
Crystal system	monoclinic	triclinic
Space group	$P2_1/c$ (No. 14)	$P\bar{1}$ (No. 2)
a [Å]	17.9797(16)	10.2613(12)
b [Å]	8.7315(12)	11.807(2)
c [Å]	20.390(5)	19.428(3)
α [°]	90	97.598(8)
β [°]	122.084(12)	94.227(10)
γ [°]	90	103.319(10)
V [Å^3]	2712.1(9)	2257.1(6)
$D_{calcd.}$ [g cm^{-3}]	1.538	1.426
Z	4	1
F (000)	1272	990
μ [mm^{-1}] (Mo-K_α)	0.9	0.8
Crystal colour	yellow	pale yellow
Crystal size [mm]	0.15 × 0.25 × 0.40	0.05 × 0.15 × 0.15
Data collection:		
θ_{min}, θ_{max} [°]	1.6, 27.5	0.9, 25.4
X-ray exposure [h]	1.5	4
Data set	−23:23, −11:9, −23:26	−12:12, −14:13, −18:23
Total data	21995	15846
Total unique data	6192	8259
R_{int}	0.0396	0.0601
R_σ	0.0370	0.0757
Absorption corr. range	0.953, 1.027 [MULTI-SCAN][a]	−
Refinement:		
No. of refined parameters	409	415
Final $R1$[b]	0.0291 [5013 $I > 2\sigma(I)$]	0.0442 [6653 $I > 2\sigma(I)$]
Final $wR2$[c]	0.0823	0.1171
Goodness of fit	1.075	1.021
w^{-1}[d]	$\sigma^2(F^2) + (0.0327P)^2 + 1.81P$	$\sigma^2(F^2) + (0.0589P)^2$
$(\Delta/\sigma)_a$, $(\Delta/\sigma)_{max}$	< 0.001, 0.001	< 0.001, 0.001
Min. and max. residual density [e$^-$ Å^{-3}]	−0.50, 0.64	−0.52, 0.83

[a] Incorporated in PLATON.[22] − [b] $R1 = \Sigma||F_o| - |F_c||/\Sigma|F_o|$. − [c] $wR2 = [\Sigma[w(F_o^2 - F_c^2)^2]/\Sigma[w(F_o^2)^2]]^{1/2}$. − [d] $P = [\mathrm{Max}(F_o^2, 0) + 2F_c^2]/3$.

δ = 1.29 [s, 36 H, $C(CH_3)_3$], 4.04 (s, 8 H, CH_2S), 6.92 (s, 2 H, Ar H), 7.19 (d, *J* = 8.6 Hz, 8 H, SAr), 7.27 (d, *J* = 8.6 Hz, 8 H, SAr). − ^{13}C NMR: δ = 31.3, 34.5, 36.7, 130.8, 132.4, 132.8, 134.9, 150.1. − FAB-MS; *m/z*: 625.2 [M − SAr]$^+$, calcd. 625.3. − $C_{50}H_{62}S_4$·0.5H_2O: calcd. C 75.04, H 7.93, S 16.03; found C 75.01, H 7.86, S 15.90.

Bis(acetonitrile) Complex of Pd Dipincer 3: Dipincer ligand **6** (213 mg, 0.3 mmol) was dissolved in CH_3CN (40 mL) and the solution was placed under argon. $Pd[MeCN]_4(BF_4)_2$ (240 mg, 0.6 mmol) was added in one portion, and the mixture was heated at reflux overnight. After evaporation of the solvent, the crude product was taken up in CH_3CN (5 mL) and precipitated by dropwise addition of Et_2O. Yield: 203 mg (60%). − M.p. > 280 °C (dec.). − ^{1}H NMR (CD_3CN): δ = 1.33 [s, 36 H, $C(CH_3)_3$], 4.61 (br s, 8 H, CH_2S), 7.56 (d, *J* = 8.8 Hz, 8 H, SAr H), 7.74 (d, *J* = 8.8 Hz, 8 H, SAr H). − ^{13}C NMR (CD_3CN): δ = 30.8, 35.2, 50.0, 127.8, 127.9, 132.0, 145.8, 155.2. − FAB-MS; *m/z*: 1001.1 [M − 2MeCN − 2BF_4 + H]$^+$, calcd. 1001.2. − $C_{52}H_{65}B_2F_8NOPd_2S_4$·2$H_2O$: calcd. C 49.15, H 5.47, N 1.10 S 10.09; found C 48.86, H 5.14, N 1.25, S 10.00 (the found values for the elemental composition correspond to the substitution of one acetonitrile ligand by water, which probably occurs upon prolonged standing).

Crystal Structure Determinations of 1 and 3·$(PPh_3)_2$: Crystals suitable for X-ray structure determination were mounted on a Lindemann-glass capillary and transferred into the cold nitrogen stream of the diffractometer. Data were collected with a Nonius Kappa CCD diffractometer on rotating anode (Mo-K_α radiation, graphite monochromator, λ = 0.71073 Å, *T* = 150 K, φ and ω scans). Pertinent data for the structure determinations are collected in Table 4. Structures were solved with automated Patterson and subsequent difference Fourier methods for structure **1** and direct methods for structure **3**·$(PPh_3)_2$, using SHELXS86[20] for both structures. Full-matrix refinement on F^2 was performed with SHELXL-97−2.[21] The hydrogen atoms of structure **1** were located on a difference Fourier map and their coordinates were included as parameters in the refinement; the hydrogen atoms of **3**·$(PPh_3)_2$ were included in the refinement on calculated positions riding on their carrier atoms. The nonhydrogen atoms were refined with anisotropic displacement parameters. The hydrogen atoms were refined with a fixed isotropic displacement parameter related to the value of the equivalent isotropic displacement parameter of their carrier atoms. The *t*Bu groups of **3**·$(PPh_3)_2$ were refined with a disorder model involving two sites. The BF_4^- counteranions and the chloroform solvent molecules of this compound were also disordered. Since no satisfactory disorder model could be obtained the contribution of the disordered region to the structure factors was taken into account using the SQUEEZE procedure as incorporated in PLATON.[22] A total of 219 e^- were found in a cavity of 537 Å^3, located at the inversion center on (0,0,0). Neutral atom scattering factors and anomalous dispersion corrections were taken from the International Tables for Crystallography.[23] Geometrical calculations were performed with PLATON.[22] Crystallographic data (excluding structure factors) for the structures reported in this paper have been deposited with the Cambridge Crystallographic Data Centre as supplementary publication nos. CCDC-141832 [for **3** · $(PPh_3)_2$] and -141833 (for **1**). Copies of the data can be obtained free of charge on application to CCDC, 12 Union Road, Cambridge CB2 1EZ, UK [Fax: (internat.) + 44-1223/336-033; E-mail: deposit@ccdc.cam.ac.uk].

Acknowledgments

Financial support of this research by the Council for the Chemical Sciences of the Netherlands Organization for Scientific Research (CW-NWO) is gratefully acknowledged.

[1] These tridentate ligands are usually abbreviated as NCN, PCP and SCS ligands.
[2] [2a] A. Weisman, M. Gozin, H.-B. Kraatz, D. Milstein, *Inorg. Chem.* **1996**, *35*, 1792, and references cited therein. − [2b] P. Steenwinkel, R. A. Gossage, G. van Koten, *Chem. Eur. J.* **1998**, *4*, 759, and references cited therein.
[3] Only one Pt^{II} SCS pincer complex has been reported: G. S. Hanan, J. E. Kickham, S. J. Loeb, *J. Chem. Soc., Chem. Commun.* **1991**, 893.
[4] [4a] J. E. Kickham, S. J. Loeb, S. L. Murphy, *Chem. Eur. J.* **1997**, *3*, 1203 − [4b] J. R. Hall, S. J. Loeb, G. K. H. Shimizu, G. P. A. Yap, *Angew. Chem. Int. Ed.* **1998**, *37*, 121.
[5] Recent reviews on metallodendrimers: [5a] G. R. Newkome, E. He, C. N. Moorefield, *Chem. Rev.* **1999**, *99*, 1689 − [5b] M. A. Hearshaw, J. R. Moss, *Chem. Commun.* **1999**, 1. − [5c]C. Gorman, *Adv. Mater.* **1998**, *10*, 295.
[6] W. T. S. Huck, F. C. J. M. van Veggel, D. N. Reinhoudt, *Angew. Chem. Int. Ed. Engl.* **1996**, *35*, 1213.
[7] [7a] W. T. S. Huck, F. C. J. M. van Veggel, B. L. Kropman, D. H. A. Blank, E. G. Keim, M. M. A. Smithers, D. N. Reinhoudt, *J. Am. Chem. Soc.* **1995**, *117*, 8293. − [7b] W. T. S. Huck, F. C. J. M. van Veggel, D. N. Reinhoudt, *J. Mater. Chem.* **1997**, *7*, 1213.
[8] W. T. S. Huck, L. J. Prins, R. H. Fokkens, N. M. M. Nibbering, F. C. J. M. van Veggel, D. N. Reinhoudt, *J. Am. Chem. Soc.* **1998**, *120*, 6240.
[9] J. E. Kickham, S. J. Loeb, *Inorg. Chem.* **1994**, *33*, 4351.
[10] For example, see: M. Fujita, F. Ibukuro, H. Hagihara, K. Ogura, *Nature* **1994**, *367*, 720.
[11] M. L. Tobe, J. Burgess, *Inorganic Reaction Mechanisms*, Longman, Essex, **1999**.
[12] M. Oki, "Applications of Dynamic NMR Spectroscopy to Organic Chemistry", *Methods in Stereochemical Analysis*, vol. 4, VCH, Weinheim, **1985**.
[13] H. C. Brown, Y. Okamoto, *J. Am. Chem. Soc.* **1958**, *80*, 4979.
[14] M. Gozin, A. Weisman, Y. Ben-David, D. Milstein, *Nature* **1993**, *364*, 699.
[15] R. A. T. M. Abbenhuis, I. Del Río, M. M. Bergshoef, J. Boersma, N. Veldman, A. L. Spek, G. van Koten, *Inorg. Chem.* **1998**, *37*, 1749.
[16] J. Errington, W. S. McDonald, B. L. Shaw, *J. Chem. Soc., Dalton Trans.* **1980**, 2312.
[17] S. J. Loeb, G. K. H. Shimizu, *J. Chem. Soc., Chem. Commun.* **1993**, 1395.
[18] C. A. Tolman, *Chem. Rev.* **1977**, *77*, 313.
[19] Isothiocyanates were found to be too weak to displace the acetonitrile from complex **1**. In the ^{1}H NMR spectrum ($CDCl_3$), the diagnostic signal shift from δ = 2.08 (coordinated CH_3CN) to δ = 1.99 (uncoordinated CH_3CN) was not observed upon addition of butyl isothiocyanate to the acetonitrile complex **1**. FT-IR spectroscopy also failed to demonstrate the coordination of isothiocyanate to Pd^{II}.
[20] G. M. Sheldrick, *SHELXS86 Program for crystal structure determination*, University of Göttingen, Germany, **1986**.
[21] G. M. Sheldrick, *SHELXL-97−2 Program for crystal structure refinement*, University of Göttingen, Germany, **1997**.
[22] A. L. Spek, *PLATON, A multi-purpose crystallographic tool*, Utrecht University, The Netherlands, **2000**; Internet: http://www.cryst.chem.uu.nl/platon/
[23] A. J. C. Wilson (Ed.), *International Tables for Crystallography*, vol. C, Kluwer Academic Publishers, Dordrecht, The Netherlands, **1992**.

Received March 21, 2000
[I00103]